Title

A Model for the Characterization of the Polarizability of Thin Films Independently of the Thickness of the Film

Journal

The Journal of Physical Chemistry B, 122(2)

ISSN

1520-6106

Authors

Sacha, GM
Verdaguer, A
Salmeron, M

Publication Date

2018-01-18

DOI

10.1021/acs.jpcb.7b06975

Peer reviewed

A model for the characterization of the polarizability of thin films independently of the thickness of the film

G. M. Sacha.
Universidad Autónoma de Madrid. Campus de Cantoblanco. 28049 Madrid, Spain
A. Verdaguer.
Institut de Ciència de Materials de Barcelona ICMAB-CSIC, Campus de la UAB, 08193 Bellaterra, Spain
M. Salmeron.
Materials Science Division. Lawrence Berkeley National Laboratory.
94720 Berkeley, CA.

The dielectric properties of thin films can be modified relative to the bulk material because the interaction between film and substrate influences the mobility of the atoms or molecules in the first layers. Here we show that a strong scale effect occurs in nanometer size octadecylammine thin films. This effect is attributed to the different distribution of molecules depending on the size of the film. To accurately describe this effect, we have developed a model which is a reinterpretation of the linearized Thomas-Fermi approximation. Within this model, we have been able to characterize the polarizability of thin films independently of the thickness of the film.

Introduction

The ability to control electronic properties of a material at the nanoscale is at the heart of modern science. High precision quantitative characterization of thin films is an essential topic for the developing of new technologies. Metallic transistors that could be scaled down to much smaller sizes would consume less energy and operate at higher frequencies than traditional semiconducting devices[1]. Biology is also finding in the nanoworld new possibilities to control systems within a molecular scale. Organic conductors are examples of nontraditional materials used to create thin films in a limit where metal or semimetal are thermodynamically unstable[2]. Non-volatile memories that use ferroelectric thin films[3] or the solar cells technology[4] are examples of topics where the miniaturization to the nanometer scale is also having a great importance.

Traditionally, a standard technique to obtain the permittivity or other electronic properties was the parallel plate capacitor, where the dielectric material is inserted between the plates. The main problem of this technique is that the method becomes unstable when the distance between the plates is very small. X-ray microdiffraction[5] or microscopic probes[6] are useful techniques to analyze electronic properties at the sub-micrometer scale. It has been common to use also the Scanning Electron Microscopy (SEM)[7], Transmission Electron Microscopy (TEM)[8], Field-Ion Microscopy (FIM)[9], Scanning Capacitance Microscopy[10,11] and different Scanning Probe Microscopies (SPM)[12].

One of the most useful SPM techniques in the characterization of thin films is Electrostatic Force Microscopy (EFM)[13]. The long-range nature of electrostatic forces is a key factor for obtaining accurate measurements at very different tip-sample distances. This fact gives EFM a great versatility when measuring at very different experimental conditions. For example, EFM has demonstrated to be useful when measuring soft biological samples without damaging them.[14,15] The long-range nature of the electrostatic forces also implies that the microscopic elements of the tip[16] and the substrate below the sample[17] should be considered in the data analysis.

One of the key factors of the EFM technique is the long-range nature of the electrostatic forces, which allows us to obtain a clear signal of the interaction between tip and sample at a distance larger than 10 nm. As we will show, the resolution obtained is enough to characterize thin films a few nanometers thick (≈5 nm), when measuring at tip-sample distances of 10 nm or more.

By using EFM we demonstrate here that a very high effect of the scale can been found when the size of thin films is smaller than a few nanometers. A difference of a factor 3 on the dielectric constant has been found in octadecylammine thin films when the size changes from 20 to 1.7 nm. As we will discuss, this effect can be attributed to the penetration of the electric field through the film thickness and its effect on the substrate below.

First, we will show experimental evidence of the dependence of the dielectric constant with the thin

film thickness. Then we will propose a model where the different polarizability of the molecules as a function of the thin film thickness is taken into account. We will also demonstrate that our model perfectly fits our previous experimental data.

Theoretical simulations

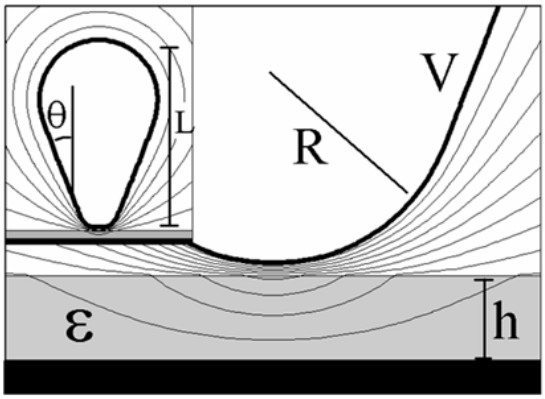

Figure 1: Equipotential distribution of a tip-sample system for a typical AFM geometry. The sample is a metallic samiinfinite plate with a dielectric thin film over the surface.

In our simulations, the tip-sample system consists on a thin film with thickness *h* and dielectric constant ε, placed on a grounded metallic electrode (see figure 1). The cantilever-tip system consists of a flat cantilever supporting a quasi-conical tip characterized by three parameters: the apex radius *R*, the semi-angle θ and the total length *L*. A voltage *V* is applied to the cantilever-tip system with its apex placed at a distance *D* from the thin film surface. z and ρ will be defined as the vertical and lateral coordinates respectively. In a standard EFM geometry, the cantilever area will be much greater than L, and h will be much smaller. Within these limits, previous results have shown that the cantilever part contributes only as a constant value to the force[18].

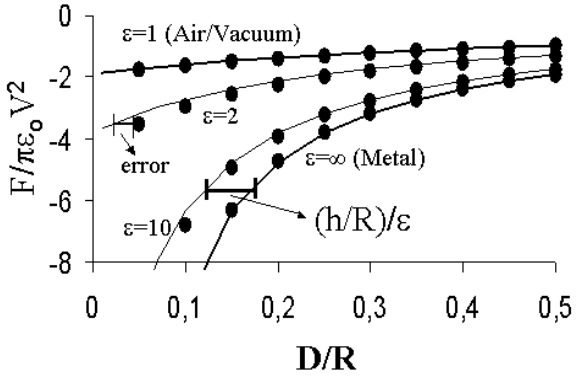

Figure 2: Normalized electrostatic force as a function of the tip-sample distance calculated by the GICM (dots) and by eq [2] (continuous line). Force has been obtained for ε=∞ (metallic sample) ε=10, ε=2 and ε=1 (Air/Vacuum). h=0.5R.

To analyze the electrostatic interaction we calculate the surface charge density on the tip and sample with the Generalized Image Charge Method (GICM)[19]. Using this technique, the surface charge density is replaced by a set of *N* point charges and *M* segments of length L_i along the tip axis. The electrostatic potential can then be calculated by the following expression:

$$V(r) = \sum_{i}^{N+M} \frac{q_i}{\varepsilon_0} G(r, r_i; L_i, h, \varepsilon) \qquad [1]$$

where *G* is the Green function of the segments and punctual charges including the polarization (response) of the sample. In our case, consisting of a dielectric thin film over a metallic sample (figure 1), *G* will be an infinite sum of image charges[20]. The final value of q_i is obtained after a standard least-squares minimization fitting the boundary condition *V* at the tip surface. Once we know the parameters, the force and force gradient can be calculated from the coulomb interaction or from the derivatives of the capacitance. This technique is able, in contrast with other numerical methods, to support differences of several orders of magnitude in the geometry without a high increase of computation time. This is very useful for systems like a standard EFM setup, where distances between microns (tip length) and nanometers (tip-sample distance) are mixed.

Figure 2 shows the normalized force as a function of D obtained by the GICM. The force has been obtained for h=0.5R and different dielectric constants. Both the metallic and Air/vacuum limits correspond to a tip over a metallic sample with different tip-sample distances (D and D+h respectively). The behaviour of the force is well known for metallic samples[21]. Taken into account these previous results and the boundary conditions of a dielectric plate, a simple expression can be deduced for the electrostatic force:

$$F \approx F_{macro} - \pi\varepsilon_0 V^2 \frac{R}{D + h/\varepsilon} \qquad [2]$$

where F_{macro} is the contribution of the macroscopic shape of the tip (L, θ and the cantilever). Figure 2 shows also (continuous line) the Force obtained with equation [2]. The metallic sample can be easily obtained in two limits: ε=∞ or h=0. Air/Vacuum can be simulated with ε=1.

Analyzing equation [2] we can see that the thin film displaces the F vs D curve from the one obtained over a metallic sample. The horizontal distance between the two curves is h/ε. (figure 2). This approximation allows us to obtain a quantitative value of h/ε measuring the horizontal distance between the target curve and the one obtained from a metallic sample.

Being the spring constant a factor of proportionality between force and tip deflection, h/ε can be directly obtained from both measurements. The condition to use the tip deflection instead of the force is that the spring constant and tip radius must be the same both for metallic and thin film sample. The only way to be sure is to use the same tip. It is also worth noticing that h/ε is a factor where topography and dielectric

properties are mixed, in line with the well-known concept of equivalent surface profile[22].

Equation [2] is a theoretical approximation from the exact electrostatic force, so an error intrinsic to the theory exists. The horizontal distance between dots (exact calculation) and the continuous line (approximation) in figure 2 is a good estimation of this error. The normalized error increases when the tip-sample distance decreases. That implies that the maximum error will occur at the closest tip-sample distance. This distance is the jump-to-contact distance D_{jtc} and it will be determined by the mechanical instability of the cantilever when the electrostatic force is applied. If the cantilever is considered a harmonic oscillator, D_{jtc} can be obtained from $K=dF_{elec}/dD$ where K is the spring constant and F_{elec} the electrostatic force) It may also be produced by the formation of a water bridge between tip and sample[23]. The error increases when h increases and ε decreases and it vanishes when $h\rightarrow 0$ and $\varepsilon\rightarrow\infty$. At these two points we will be limited by the experimental noise. The error has been analyzed for K up to 10 N/m and R up to 100nm and it has been found to be always smaller than a 20%, We use the following limiting values: ε(2,∞) and R(20,100nm) in the analysis.

Dielectric constant estimation

Experiments to analyse the dielectric constant at the nanoscale have been made with TiN-coated Ultrasharp Si tips from Mikromash, Inc. The goal of the experiments is to obtain the dielectric constant using the same sample for both metallic and thin film regions. The metallic sample, gold on mica (10x10mm), was made using a Denton Vacuum metal evaporator and annealed by butane flame before use[24]. The dielectric thin film is octadecylamine (ODA, Fluka, >99% purity), which was prepared over the gold surface from 15nM ethanol solutions (Aldrich, HPLC grade). The gold sample was dipped into the ODA solution for few minutes, rinsed twice with pure ethanol and dried under nitrogen. The *F* versus *D* curves were obtained with an Asylum MFP-3D AFM. The spring constant of the cantilever was obtained from the thermal noise spectrum using the software provided with the MFP-3D instrument. Octadecylamine ($C_{18}H_{37}NH_2$) from Fluka (>99%) was used as received with no further purification. Experiments were performed in an environmental control chamber with dry nitrogen flowing in the chamber with a RH <5%. This low humidity prevents the formation of water bridges due to the water adsorbed on the surface. On the other hand, octadelamine has an hydrophobic and a hydrophilic end where multilayer films have always an hydrophobic end at the surface (monolayer with hydrophilic end on gold and then bilayers on top of that) which prevents large amount of water to adsorb on the surface.

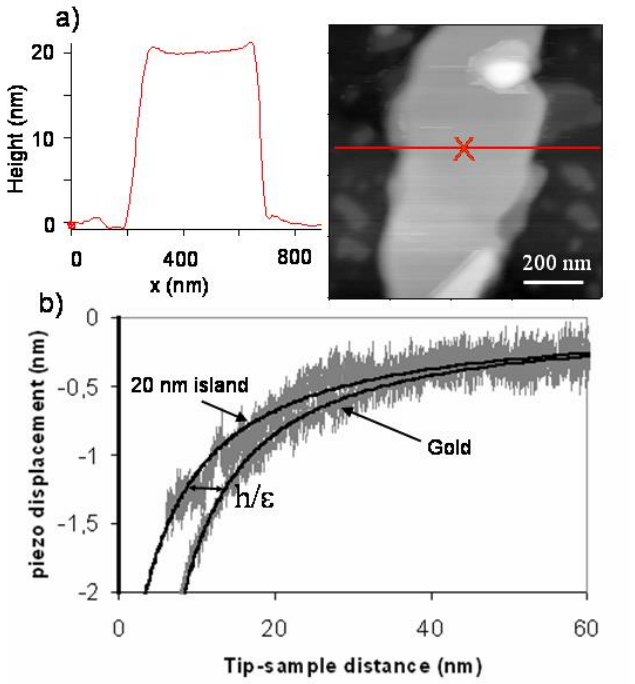

Figure 3: a) Surface profile and topography of a 20 nm island on the gold surface. Profile has been taken along the line shown in the topographic image. b) Piezo displacement as a function of distance over the metallic (gold) surface and over the dielectric island (exact position indicated on the topography by a cross). Continuous line shows the force obtained by eq [2]. V=10V.

Depending on the immersion time multilayers of ODA were observed on the gold surface. Figure 3a shows a profile and a topographic image of a flat 20 nm thick ODA multilayer island (12-15 monolayers considering that the thickness of the first tilted monolayer is found to be between 1.3 nm and 1,7 nm on mica while the length of the molecule is 2.46 nm[25]) island has been created (grey region in the middle of the image). The island is larger than 400 nm, allowing us to obtain *F* vs D curves without boundary effects. The black region is the clean gold surface. The bottom of the image shows the tip deflection as a function of the tip-sample distance over clean gold and over the ODA island at the position marked by the red cross. A value of 12.5 N/m was obtained for the spring constant of the cantilever. Using the piezo displacement and the spring constant of the cantilever, an effective electrostatic tip radius of 75±10 nm has been obtained following the method shown in reference[26].

Using the surface profile, we can obtain a value for the island thickness: h=20±1 nm (error taken directly from the profile). Figure 3b shows the tip deflection as a function of the tip-sample distance. Dark continuous line shows the best fit using eq [2] for both metallic and thin film samples. The distance between these two curves is h/ε=5±1nm (error due to experimental noise). Using h/ε and the island thickness obtained from the surface profile, we can determine the dielectric constant value ε=4.21±1.04 (error about

25%). This value (obtained with V=10 V) was confirmed with experiments at 6 and 8 V bias.

Dipping the gold surface into the ODA solution for a shorter time we obtain islands of smaller thickness. Figure 4 shows a gold sample (dark grey) with several 5±0.5 nm (2-3 Monolayers) islands (light grey). The size of clean gold and island is enough in some regions to consider a flat infinite surface (i.e. no boundary effects). Numbers indicate the regions where the F vs D curves have been taken. Using the same approximation, a value h/ε=3.5±0.2 is obtained. This value, together with the island thickness gives ε=1.44±0.22 (error about 15%).

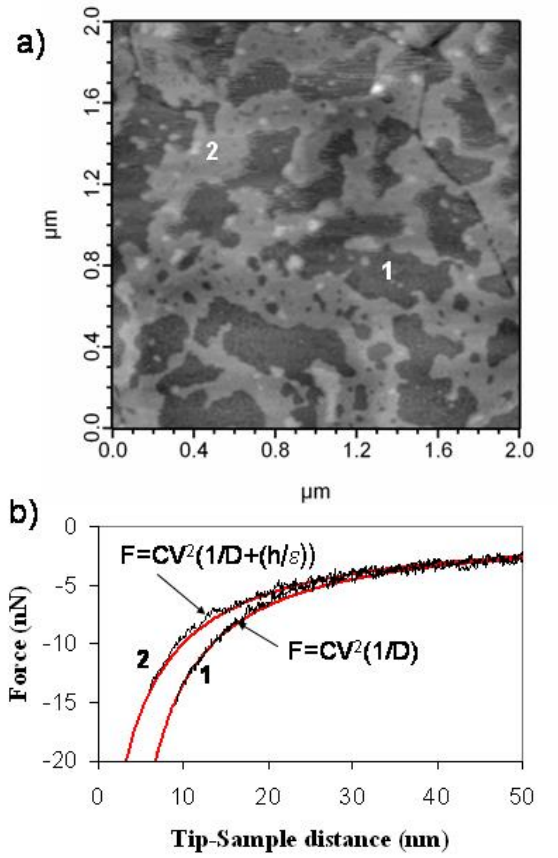

Figure 4: a) Topography image of a clean gold surface (dark) with several 5 nm octadecylammine islands (light grey). b) Force as a function of tip-sample distance for gold (1) and 5 nm islands (2). V=6V, R=135nm.

In figure 5a we show a sample where ODA islands of four different thickness are found. The islands have enough extension to avoid lateral effects (i.e. we can consider the sample an infinite thin film as we did when analysing results from figure 3). In this case, we can see that the estimated dielectric constant of the thin film increases as we increase the number of layers included in the film. As we can see in figure 5, the apparent dielectric constant almost doubles when the number of layers increases from 1 to 10.

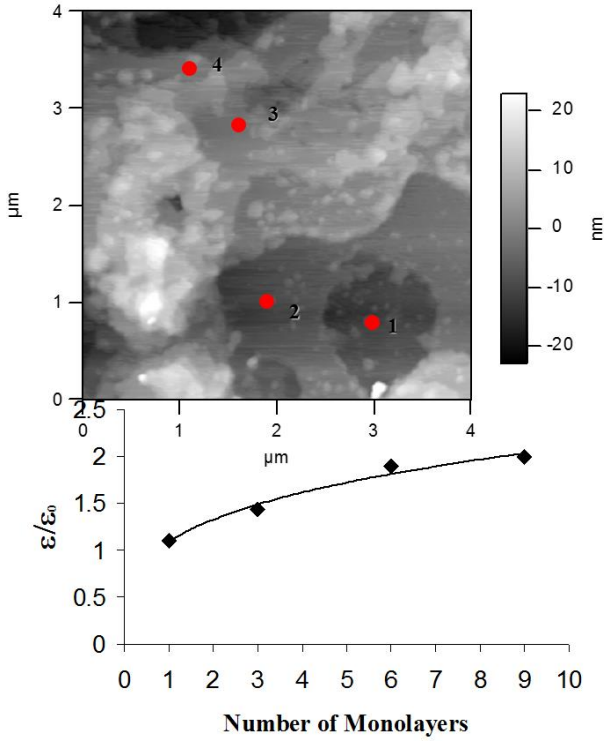

Figure 5: a) Topography image of a gold surface with an octadecylamine film exposing regions of different thickness. Numbers indicate the number of octadecylamine layers. b) Dielectric constant measurement for the four different thickness (number of molecular layers).

Discussion

In previous section, we have observed that the apparent value of the dielectric constant is much smaller for thin octadecylammine islands (ε between 1 and 2) than for 20 nm island (4.21±1.04). Being the same molecule in all cases, we must assume that the dielectric constant is affected by the thickness of the film. To explain this we assume that the first layers attached to the surface have a smaller ability to change orientation when an electric field is applied, so that they do have a smaller dielectric constant. On the other side, in the islands with 12-13 layers (20 nm) the molecules farther away from the gold surface have a better ability to reorient in response to the electric field, as expected also from the high dipole of the ODA molecules.[27]

To get an accurate calculation of the electric field inside the thin films under these conditions, we propose to include the gradient of the mobility inside the thin film by following the model proposed in [28], where the sample conductivity is included through a simple linearized Thomas-Fermi (Debby-Hückel) approximation. In this model, the electrostatic potential is obtained by solving the following expression:

$$\nabla^2 V_i(r) - \frac{1}{\lambda_i^2} V_i(r) = 0 \qquad (3)$$

where λ is the screening length. In the dielectric thin films analyzed here, λ is a parameter that takes into

account the mobility of the molecules as a function of their position inside the thin film. Similar interpretation has been proposed before when measuring the dielectric constant as a function of the thickness inside a capacitor.[29,30] This model has been also used to study double layer or semiconductor physics. All of these problems are related somehow with finite charge mobility and that is the reason why we propose that it can be also used to simulate the different polarizability of the molecules as a function of the thin film thickness. Essentially, what we have here is a polarizability that changes with the thickness. The molecules that are closer to the surface, have a stronger polarizability, and we propose that it can be simulated as a screening length induced by a finite amount of free charge.

The electrostatic potential for a single point charge q located in region i=0 at (z=0, ρ=0), can be written as

$$V_i = \frac{q}{4\pi\varepsilon_0}\left[\int_0^\infty J_0(k\rho)\left(\psi_i(k)e^{-K_z z} + \theta_i(k)e^{K_z z}\right)dk\right] \quad (4)$$

where $K_z^2=k^2-1/\lambda_i^2$, J_0 are the first order Bessel functions and ψ_i and θ_i are coefficients obtained by applying the electrostatic boundary conditions ($V_i=V_{i+1}$ and $\varepsilon_i V'_i=\varepsilon_{i+1}V'_{i+1}$ at $z=z_{i,i+1}$) to the sample interfaces [24]. To calculate the electrostatic potential at the tip surface, the GICM can be used as in the previous model.

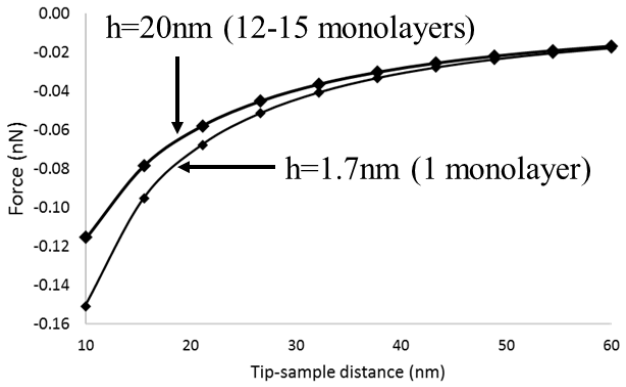

Figure 6: Electrostatic force vs tip-sample distance for both a monolayer thin film and a thin film composed by 12-15 monolayers. Dots represent the electrostatic force for a film of dielectric constant ε=1.1 for h=1.7nm, and ε=4.21 for h=20nm. Continuous lines represent the electrostatic force when both thin films have been characterized by ε=1.1 and λ=5nm. Tip is a sphere of radius 70 nm which is connected to a 1V voltage source.

Since the mobility of the molecules is included in this model by the λ parameter, we will describe the film by an ε value equal to the smallest one found in the experimental results (ε=1.1 for h=1.7nm). This value represent the minimum polarizability of the molecules, found in the ones closely attached to the substrate. The increasing dielectric constant found by higher h values will be included in the simulations by the λ parameter.

In figure 6 we show the electrostatic force for both the standard description of the thin film (ε and h) and the new approximation that includes a fixed ε value (ε=1.1 for all h values) and a finite λ value. For λ=5nm, we can see in the figure that both models are in striking agreement for both the thinnest and thicker films found in the experiments. Intermediate values (not shown in the figure for clarity) are also in agreement with an error below 20%.

The great advantage of the new model is that two fixed values are used (ε=1.1, λ=5nm) for all h values instead of using a parameter that changes as a function of h (previously, ε increased from 1.1 to 4.21 when h increased). In other words, the new description of the thin film gives two quantitative magnitudes that are independent of the geometry (i.e. only depends on the nature of the molecules).

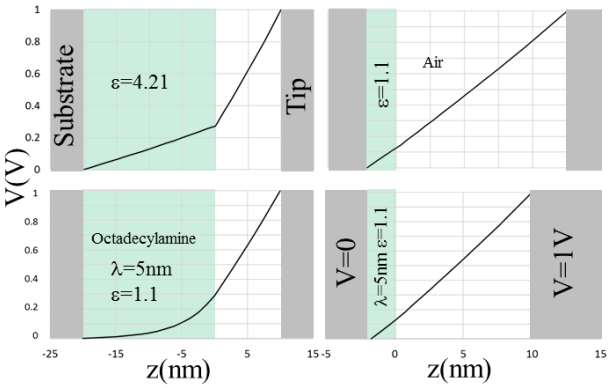

Figure 7: Voltage drop between tip and substrate for the classical thin film characterization (top) and the (λ,ε) model proposed here. Octadecylamine thin films thicknesses are 20nm (left) and 1.7nm (right).

In figure 7 we show the voltage drop between the tip apex and the substrate below the thin film for both models. As we can see, for the 1.7nm thin film (right side), there is no difference between the standard description (top) and the new model (bottom). In this case, λ is too large compared to the thin film thickness and it does not have any effect. This is the limit where the ODA molecules are strongly attached to the surface and a very small polarizability is detected (ε=1.1). On the other side, for h=20nm, we can see a large difference in the potential drop between the standard description (top) and the new model (bottom). When using the standard description, a linear potential drop is found, which is not a realistic situation since the molecules attached to the surface have much smaller polarizability. However, this fact is taken into account in the new model, where the electrostatic potential changes in a non-linear way within the thin film.

Conclusions

In this letter we have developed a simple method to obtain quantitative information about the dielectric properties of thin films, in the nanometer scale. The dielectric constant and thickness can be obtained from measurements of topographic images and

by force versus distance curves. Using this method we have shown the strong influence of the thickness of the island on the dielectric constant.

We have developed a model that is able to explain quantitatively the different values of the dielectric constant as a function of the thickness as a result of the different mobility of the octadecylamine molecules as a function of their distance to the substrate. The model allows us to describe the thin film by two parameters that do not depend on the thin film thickness. The first one is related to the minimum polarizability of the molecules and the second one is related to the gradient of mobility as a function of the relative position of the molecules within the thin film. This description of the dielectric properties of nanoscale thin films will be useful for accurately predict the dielectric response of thin films independently of their geometry.

ACKNOWLEDGEMENTS

The authors would like to thank J. J. Sáenz for helpful discussions. This work was supported by the "Self-Assembly of Organic/Inorganic Nanocomposite Materials" program, Office of Science, the Office of Basic Energy Sciences (BES), Materials Sciences and Engineering (MSE) Division of the U.S. Department of Energy (DOE) under Contract No. DE-AC02-05CH11231.

(1) Rotkin, S. V.; Hess, K. Possibility of a metallic field-effect transistor. Appl. Phys. Lett. **2004**, 84, 3139.

(2) Novoselov, K. S.; Geim, A. K.; Morozov, S. V.; Jiang, D.; Zhang, Y.; Dubonos, S. V.; Grigorieva, I. V.; Firsov, A. A. Electric Field Effect in Atomically Thin Carbon Films. Science **2004**, 306, 666.

(3) Brewer, S. J. et al. Effect of microstructure on irradiated ferroelectric thin films. J. Appl. Phys. **2017,** 121, 244102.

(4) Szyszka, A. et. al. A cross-sectional scanning capacitance microscopy characterization of GaAs based solar cell structures. Cryst. Res. Technol. **2017,** 52, 1700019.

(5) Do, D. H. et al. Structural visualization of polarization fatigue in epitaxial ferroelectric oxide devices. Nature materials **2004**, 3, 365.

(6) Gruverman, A. ; Auciello, O. ; Tokumoto, H. Imaging and control of domain structures in ferroelectric thin films via scanning force microscopy. Annu. Rev. Mater. Sci. **1998**, 28, 101.

(7) Kavitha, B.; Nirmala, M.; Poornachandra, S.; Pavithra, M. Preparation and Characterization of CdO Thin Films Prepared by Chemical Method. J. Environ. Nanotechnol. **2017**, 6, 59.

(8) Reimer, L. Transmission Electron Microscopy: Physics of Image Formation and Microanalysis. Springer series in optical sciences. **1984** v36.

(9) Tsong, T. T. Energetics of surface atomic processes and effects on growth of ultrathin films and nanoislands. Progress in Surface Science **2003**, 74, 69.

(10) LinWang, L.; Gautier, B.; Sabac, A.; Bremond, G. Investigation of tip-depletion-induced fail in scanning capacitance microscopy for the determination of carrier type. Ultramicroscopy **2017**, 174, 46.

(11) Gomila, G.; Toset, J.; Fumagalli, L. Nanoscale capacitance microscopy of thin dielectric films. J. Appl. Phys. **2008**, 104, 024315.

(12) Hu, J.; Xiao, X. D.; Ogletree, D. F.; Salmeron, M. Imaging the condensation and evaporation of molecularly thin films of water with nanometer resolution. Science **1995** 268, 267.

(13) Martin, Y.; Abraham, D. W.; Wickramasinghe, H. K. High-resolution capacitance measurement and potentiometry by force microscopy. Appl. Phys. Lett **1988**, 52, 1103.

(14) Van der Hofstadt, M.; Fabregas, R.; Biagi, M. C.; Fumagalli, L.; Gomila, G. Nanoscale dielectric microscopy of non-planar samples by lift-mode electrostatic force microscopy. Nanotechnology **2016,** 27, 405706.

(15) Marliere, C.; Dharhi, S. An in vivo study of electrical charge distribution on the bacterial cell wall by atomic force microscopy in vibrating force mode. Nanoscale **2015**, 7, 8843-8857.

(16) Gramse, G.; Gomila, G.; Fumagalli, L. Quantifying the dielectric constant of thick insulators by electrostatic force microscopy: effects of the microscopic parts of the probe. Nanotechnology. **2012**, 23, 205703.

(17) Labardi, M.; Barsotti, J.; Prevosto, D.; Capaccioli, S.; Roland, C. M.; Casalini, R. Extended model for the interaction of dielectric thin films with an electrostatic force microscope probe. J. Appl. Phys. **2015**, 118, 224104.

(18) Sacha, G. M.; Saenz, J. J. Cantilever effects on electrostatic force gradient microscopy. J. Appl. Phys. Lett. **2004**, 85, 2610 (2004).

(19) Sacha, G. M. Influence of the Substrate and Tip Shape on the Characterization of Thin Films by Electrostatic Force Microscopy. IEEE Trans. Nanotechnology. **2013**, 12, 152.

(20) Smythe, W. R. Static and dynamic electricity. McGraw-Hill, New York. **1968**

(21) Castellano-Hernandez, E.; Moreno-Llorena, J.; Saenz, J. J.; Sacha, G. M. Enhanced dielectric constant resolution of thin insulating films by electrostatic force microscopy. J. Phys.: Condens. Matter **2012**, 24, 155303.

(22) Xu, L.; Salmeron, M. Studies of Wetting and Capillary Phenomena at Nanometer Scale with Scanning Polarization Force Microscopy. Nano-Surface Chemistry. **2001**, 6.

(23) Bartosik, M. et al. Nanometer-Sized Water Bridge and Pull-Off Force in AFM at Different Relative Humidities: Reproducibility Measurement and Model Based on Surface Tension Change. J. Phys. Chem. B. **2017**, 121 (3), pp 610–619

(24) Benítez, J. J.; San-Miguel, M. A.; Domínguez-Meister, S.; Heredia-Guerrero, J. A.; Salmeron, M. Structure and Chemical State of Octadecylamine Self-

Assembled Monolayers on Mica. J. Phys. Chem. C, **2011**, 115, 19716–19723.
(25) Oviedo, J.; San-Miguel, M. A.; Heredia-Guerrero, J. A.; Benitez, J. J. Electrostatic Induced Molecular Tilting in Self-Assembled Monolayers of n-Octadecylamine on Mica. J. Phys. Chem. C. **2012**, 116, 7099–7105
(26) G. M. Sacha, G. M.; Verdaguer, A.; Martínez, J.; Sáenz, J. J.; Ogletree, D. F.; Salmeron, M. Effective tip radius in electrostatic force microscopy. Appl. Phys. Lett. **2005**, **86**, 123101.
(27) Benitez, J. J.; Rodriguez, O.; Diez-Perez, I.; Sanz, F.; Salmeron, M. Dielectric properties of self-assembled layers of octadecylamine on mica in dry and humid environments. **2005,** 123, 104706.
(28) Castellano-Hernández, E.; Sacha, G. M. Finite Conductivity Effects in Electrostatic Force Microscopy on Thin Dielectric Films: A Theoretical Model. Advances in Condensed Matter Physics. **2015** 754098.
(29) Natori, K.; Otani, D.; Sano, N. Thickness dependence of the effective dielectric constant in a thin film capacitor. Appl. Phys. Lett. **1998,** 73, 632.
(30) Hwang, C. S. Thickness-dependent dielectric constants of (Ba,Sr)TiO_3 thin films with Pt or conducting oxide electrodes. J. Appl. Phys. **2002**, 92, 432.